

Analysis of GRACE Range-Rate Time Series during Strong Earthquakes: A Case Study in Iran

Moradi, A. R.¹  | Ghaffari Razin, S. R.¹  | Moradian, M.² 

1. Department of Surveying Engineering, Faculty of Geoscience Engineering, Arak University of Technology, Arak, Iran.

2. Center for Higher Education Yasin, Borujerd, Iran.

Corresponding Author E-mail: a-moradi@arakut.ac.ir

(Received: 29 July 2023, Revised: 23 Oct 2023, Accepted: 9 Jan 2024, Published online: 20 Feb 2024)

Abstract

The applicability of the Gravity Recovery and Climate Experiment (GRACE) level 1B range-rate data to detect gravity changes caused by significant earthquakes (M6.0-6.9) has been investigated. The most common product of the GRACE mission is the level 2, science data, as the spherical harmonic Stokes' coefficients of the geopotential. These coefficients have been generated from Level 1B data, resulting in missing some information during the smoothing process. In this study, the GRACE level 1B K-band range-rate measurements over three selected cells in Iran were analyzed, including two cells containing the epicenters of the Borujerd earthquake (6.1 Mw) and the Zarand earthquake (6.4 Mw), which occurred on March 31, 2006, and February 22, 2005, respectively, and one cell far enough from those two cells. Additionally, the range-rate time series attributed to Iran's main catchments containing the aforementioned zones have been extracted to distinguish between the impacts of earthquakes and hydrology on the range-rate time series. Besides, the impact of factors other than earthquakes, such as tides and non-gravitational accelerations acting on the GRACE satellites has been corrected. To better explore the extracted signals, their details have been derived using wavelet transforms, and the corresponding anomalies have been detected using the boxplot method. The considerable anomalies observed in areas within or near the epicenters of earthquakes before and after the events indicate that the GRACE and GRACE Follow-On range-rate time series can be considered as potential precursors to a major earthquake.

Keywords: GRACE, Strong earthquake, Wavelet transformation, Boxplot, Iran.

1. Introduction

Throughout history, earthquakes have endangered the lives of countless people. They have also caused significant damage to man-made structures worldwide. Throughout history, humans have tried various ways to deal with this phenomenon and mitigate its dangers. It is now widely recognized that the best way to deal with earthquakes is to secure the structures, but great efforts have been made to identify earthquake behavior and potential environmental changes before, during and after it. Numerous studies have shown that the occurrence of earthquakes can be associated with several phenomena in the environment around the epicenter, such as changes in stress and strain, in electric and magnetic fields, displacement and deformation of the Earth's crust, changes in the atmospheric and thermal environment,

emissions of gases such as radon and carbon dioxide, or changes in the Earth's gravitational field (Zhao et al., 2021). Accordingly, the International Association of Seismology and Physics of the Earth's Interior (IASPEI) considers any measurable parameters, such as the above-mentioned processes, to be known as potential earthquake precursors. The simultaneous presence of several parameters can typically be considered as a sign for earthquake prediction (Wyss, 1997). While the initial efforts related to this issue were mostly limited to environmental measurements and determination of parameters such as radon emission, ground deformation, or stress and strain changes in selected areas, today various satellite missions have made it possible to observe changes in the physical

Cite this article: Moradi, A. R., Ghaffari Razin, S. R., & Moradian, M. (2024). Analysis of GRACE Range-Rate Time Series during Strong Earthquakes: A Case Study in Iran. *Journal of the Earth and Space Physics*, 49(4), 83-92. DOI: <http://doi.org/10.22059/jesphys.2024.362018.1007540>

E-mail: (1) mr.ghaffari@arakut.ac.ir (2) mardin.moradian@gmail.com



and chemical phenomena before and after earthquakes over a wider period with greater variability.

In general, satellite missions capable of extracting data related to environmental changes caused by earthquakes can be classified into four categories. The first category includes missions whose data are used to measure electromagnetic changes before and after an earthquake. In this category, for the first time, Larkina et al. (1983) used the Interkosmos-9 satellite data to demonstrate that the intensity of electromagnetic waves at very low frequencies (between 3 and 30 Hz) increased just a few hours before an earthquake. Satellite missions, whose data are used to obtain information such as local amplitude or phase anomalies in signals with different frequencies, and the changes in the Total Electron Content (TEC), belong to this category (see, for example, Liperovskiy and Shalimov, 1983; Pulinets, 2004; Pulinets et al., 2004).

The second category provides the possibility of monitoring the changes in the Earth's surface temperature before and after earthquakes based on infrared thermal remote sensing. Zeng et al. (2009), Barkat et al. (2018), Choudhury et al. (2006), Saraf et al. (2009), and Zhong et al. (2020) are examples of this category.

The third category includes missions that provide the data necessary for analyzing and monitoring the deformation of the Earth's crust before an earthquake. Specifically, satellites such as GPS, GLONASS, and Galileo, which can estimate the deformation of the Earth's crust by determining the exact coordinates of the Earth's points and their temporal variations, are involved in these missions (See, for example, Paziewski et al., 2020; Su et al., 2018; Xiang et al., 2019; Xu et al., 2013). In addition, satellite missions such as Sentinel-1, which utilizes Interferometric Synthetic Aperture Radar (InSAR) images to monitor crustal deformation, play an important role in earthquake research in this category. In particular, a technique has been proposed to improve radar interferometry through persistent scatterer interferometric synthetic aperture radar (PS-InSAR), which can improve earthquake monitoring by achieving millimeter accuracy in determining

the crust deformation (for example, Dumka et al., 2020; Liu et al., 2021; Nardò et al., 2020).

The fourth category includes instruments used to observe changes in the Earth's gravitational field. The significant results of the Earth's gravitational field modeling based on satellite gravimetry were first achieved by the Challenging Minisatellite Payload (CHAMP) mission and subsequently improved by the Gravity Recovery and Climate Experiment (GRACE), the Gravity Field and Steady-State Ocean Circulation Explorer (GOCE), and the Gravity Recovery and Climate Experiment Follow-On (GRACE-FO). These missions are dedicated to gravity field missions due to the sharing of three important features: their extremely low and near-polar orbit, almost continuous and accurate three-dimensional positioning by GPS, and the measurement of non-gravitational accelerations, such as those caused by atmospheric drag (Rummel et al., 2002). Among them, the GRACE and GRACE-FO missions aim to monitor temporal variations in the Earth's gravity field by inter-satellite tracking between two low orbiters interconnected by a K-band microwave link to accurately measure their separation distances and their rates (Chen et al., 2022).

After the success of the GRACE mission in modeling the Earth's gravity changes from mid-2002, and then from 2018 onwards by the GRACE-FO, the data obtained from these missions has been considered as one of the sources for extracting information about large earthquakes. For the first time, Han et al. (2006) reported changes resulting from the 9.1- magnitude Sumatra- Andaman earthquake on December 26, 2004, using GRACE mission data. Since then, many studies have been conducted using the GRACE data to extract pre- or post-seismic information and to analyze the effects of earthquakes on the Earth's gravity field, two of which are the study of gravity changes due to the December 2004 (9.2 Mw) and March 2005 (8.7 Mw) Sumatra earthquakes by Panet et al. (2007), based on the continuous spherical wavelet analysis of geoid height variations from GRACE, Another significant research conducted by Shahrivand et al. (2014) to identify the gravity changes before the March 2011 (9

Mw) Japan earthquake, the February 2012 (8.8 Mw) Chile earthquake, and the April 2012 (8.6 Mw) Indian Ocean earthquake using the extracted gravity gradients from GRACE. In those studies, earthquake prediction information has been extracted based on the conventional gravity products of the GRACE mission, which are the spherical harmonic (Stokes') coefficients, available to the scientific community as Level-2 data. This type of data is obtained from the GRACE level-1B data, specifically the GRACE K-band range-rate measurements, resulting in missing information during the smoothing process (Swenson and Wahr, 2006).

Although producing and using the GRACE level1B range-rate time series is more difficult and complex than the level2 data, in this paper, the GRACE level1B range-rate time series attributed to selected areas where strong earthquakes with magnitudes between 6 and 6.9 Mw occurred. The study investigates the applicability of these data as one of the potential earthquake precursors. Previously, Moradi and Sharifi (2017) used the GRACE level1B range-rate time series to investigate the hydrological behavior of Iran's main catchments using the windowed least-squares spectral analysis. In addition, Moradi and Sharifi (2018) analyzed the GRACE range-rate time series related to the Lake Urmia basin in Iran using wavelet-based least-squares spectral analysis. In the case of earthquake studies, Han et al. (2010) utilized the GRACE level1B range-rate data to extract the spatial distribution of gravity changes following the M8.8 2010 Maule, Chile earthquake through the inversion of the GRACE range rates. Ghobadi-Far et al. (2020) utilized the GRACE level1B range rates to identify gravity changes resulting from the 2004 Sumatra, 2010 Maule, and 2011 Tohoku tsunamis. They extracted the range-rate residuals by subtracting the GRACE level1B range rates from the reference range-rate data computed from the dynamic orbits based on the necessary background models and converting the range-rate residuals to range-acceleration residuals by applying numerical differentiation. Han et al. (2011) studied the impact of gravitational variations due to the caused by the 2011 Tohoku-Oki earthquake the GRACE range-rate

measurements.

The distinguishing point of the present study is the direct analysis of the GRACE level1B range-rate time series to expand the utilization of satellite gravity data in earthquake detection; however, in previous studies, only major earthquakes with magnitudes greater than 7Mw could be detected.

The next sections of this paper are organized as follows. First, the data used in the study area, the data preparation process, and the method for extracting the time series are described. In the following section, time series will be analyzed and the results will be presented in terms of the changes caused by the selected earthquakes. Finally, the suggestions and conclusions are presented.

2. Data used, studied area and time-series extraction and analysis

The key data in this study are the inter-satellite K-band range rate (KBRR) measurements, which have an accuracy of 0.1 $\mu\text{m/s}$ and 5 seconds sampling, included in the GRACE Level1B data and cover the period from January 2004 to December 2007. Additionally, related Level-1B data products, namely the non-gravitational accelerations acting on both GRACE satellites, as measured by onboard space accelerometers (ACC1B), and the instantaneous positions of the GRACE satellites (GNV1B) during the above-mentioned period are needed for analysis purposes. A comprehensive description of the GRACE Level-1B data products can be found in Case et al. (2010).

To consider the contribution of tides to gravitational field changes, as a non-earthquake-related factor, this study models the tides according to IERS Conventions, 2010 (Petit & Luzum, 2010). Finally, the Earth Gravitational Model 2008 (EGM2008) has been used where the Earth's geopotential model has been needed for simulations (Pavlis et al., 2008).

To investigate the impact of strong earthquakes on the GRACE range-rate time series, four 1° square cells in Iran have been considered as the selected areas according to Figure 1. Cell 1 contains the epicenter of the Borujerd earthquake (6.1 Mw), which occurred on March 31, 2006 (Ramazi & Hosseinnejad, 2009). The southwest corner

of this cell is located at 33.5° latitude and 48° longitude, and cell 2 is selected adjacent to cell 1 with its southwest corner at 32.5° latitude and 48° longitude. Cell 3 is located far enough away from the epicenter of the Borujerd earthquake, with the southwest corner positioned at a latitude of 29° and a longitude of 51°. No earthquake was recorded in this cell during the Borujerd earthquake. All three above-mentioned cells have been selected within one of the main catchments of Iran, namely the Persian Gulf basin, to follow the same hydrological behavior. Cell 4 contains information about the epicenter of another strong earthquake, known as the Zarand earthquake (6.4 Mw), which occurred on February 22, 2005 (Nemati & Gheitanchi, 2011). The southwest corner of this cell, which is selected within the Central Plateau basin, another main catchment of Iran, is at 30° latitude and 56° longitude. All four cells are shown in Figure 1.

The GRACE range-rate time series related to each selected cell as well as the corresponding non-gravitational accelerations acting on each satellite, from the beginning of January 2005 to the end of December 2007, is extracted based on the GRACE Level-1B data. Similarly, the aforementioned time series can be obtained for the Persian Gulf and the Central Plateau basins. To estimate and eliminate the impact of non-gravitational accelerations on range-rate measurements, the onboard space accelerometer data must be calibrated for scale, bias, and drift parameters that affect the accelerometer measurements (Bezděk, 2010). Ignoring the effect of scaling in this study, the effects of bias and drift parameters on the accelerometer measurements are corrected using the method presented by Moradi and Sharifi (2021), which is based on the use of the discrete wavelet transform. To estimate and apply the effect of non-gravitational accelerations, the orbits of twin GRACE satellites are first estimated under

the influence of the Earth's gravitational force. In the second step, the effect of calibrated non-gravitational accelerations is added and the perturbed orbits are re-estimated. The results of the orbit generation at each step are the coordinates, and the instantaneous speed of the satellites at different times corresponding to the timespans considered previously. The simulated range-rate measurements between the two GRACE-like satellites, with and without considering the non-gravitational accelerations, can now be obtained from Equation (1) (Chen, 2007).

$$\dot{\rho} = \dot{\mathbf{r}}_{12} \cdot \mathbf{e}_{12} \quad (1)$$

In which $\dot{\mathbf{r}}_{12}$ is the relative velocity vector of two satellites and \mathbf{e}_{12} is the unique vector along the line of sight between them, where

$$\dot{\mathbf{r}}_{12} = \dot{\mathbf{r}}_2 - \dot{\mathbf{r}}_1 \quad (2)$$

and

$$\mathbf{e}_{12} = (\mathbf{r}_2 - \mathbf{r}_1) / \sqrt{(\mathbf{r}_2 - \mathbf{r}_1)^T (\mathbf{r}_2 - \mathbf{r}_1)} \quad (3)$$

The difference in the computed range-rate observations $\dot{\rho}$, once considering the effect of Earth's gravitational force and non-gravitational accelerations and on the other hand, under the influence of Earth's gravitational force only will lead to the estimation of correction values of the effect of non-gravitational accelerations on range-rate measurements at the desired times.

The effect of time-variable components on GRACE range-rate measurements, aside from earthquakes, is primarily attributed to tides and hydrological signals. These effects can be mitigated using the same way. Due to the similarity of the hydrological signals' behavior in the cells shown in Figure 1 with their corresponding catchment areas, the hydrological effect in time series has not been reduced; however, the tidal effect on the GRACE range-rates is corrected according to the procedure presented in Figure 2.

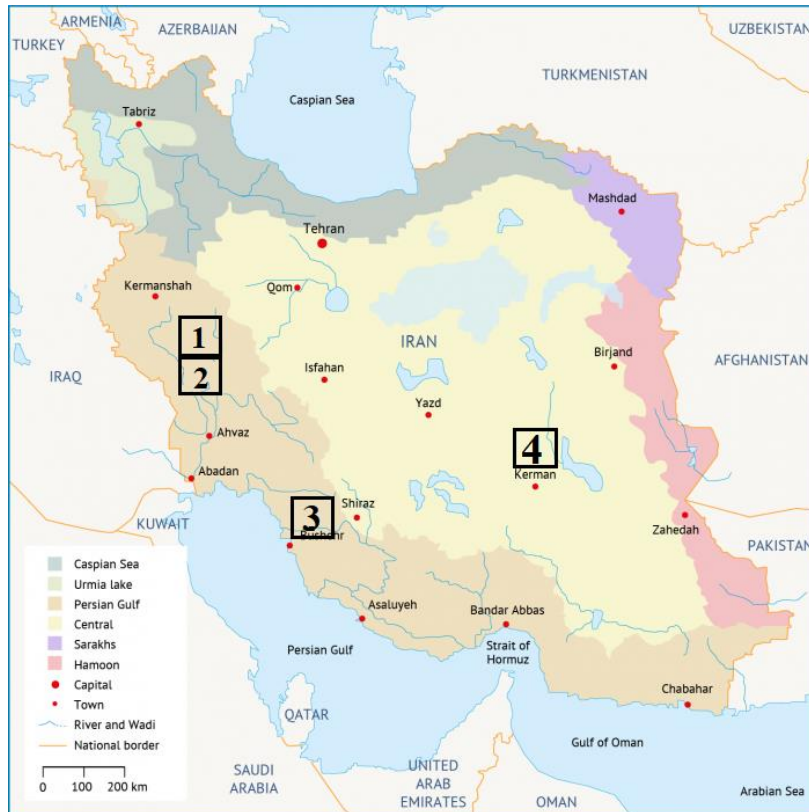


Figure 1. Six major basins of Iran (Saatsaz, 2020), along with four 1°×1° cells, as the study areas.

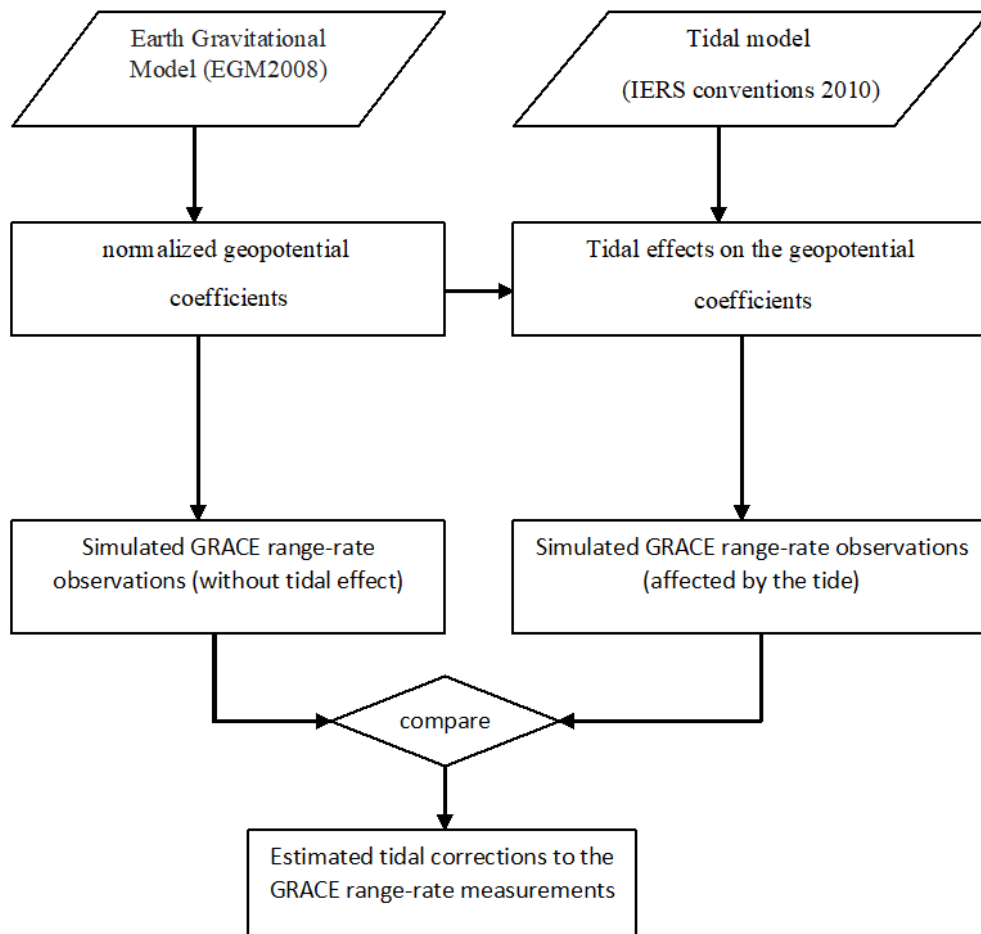


Figure 2. The process of correcting the tidal effect on the GRACE range-rate measurements.

For instance, the tidal correction time series for the Persian Gulf basin in the initial month of 2005 is calculated using the procedure mentioned above. The corresponding spectrum is then estimated using the least-squares spectral analysis method (Wells et al., 1985), which is shown in Figure 3. As expected, the principal semidiurnal components, such as the M2 component with a frequency of 1.93 cycles per day, are well

reflected in the spectrum of the estimated tidal corrections.

After applying the effects of tides and non-gravitational accelerations, the corrected monthly range-rate time series related to the selected cells in Figure 1, as well as the main catchments containing them, are extracted. These time series are presented separately in Figures 4 and 5 due to the difference in earthquake occurrence times in cells 1 and 4.

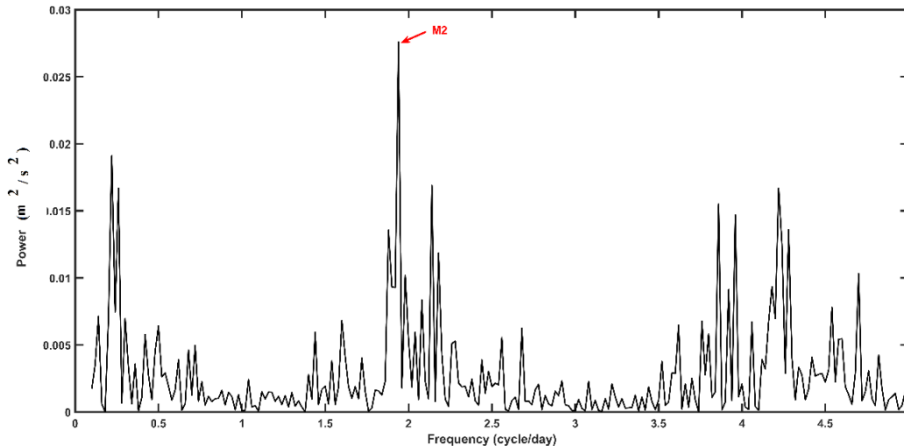


Figure 3. Least-squares power spectrum of the estimated tidal corrections to the GRACE range-rate measurements during January 2005.

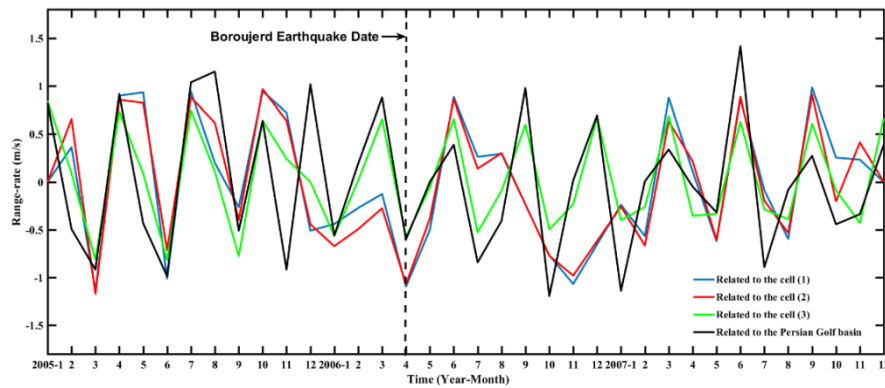


Figure 4. Corrected monthly range-rate time series related to the selected cells (1), (2), (3), and the Persian Gulf basin, from the beginning of 2005 to the end of 2007.

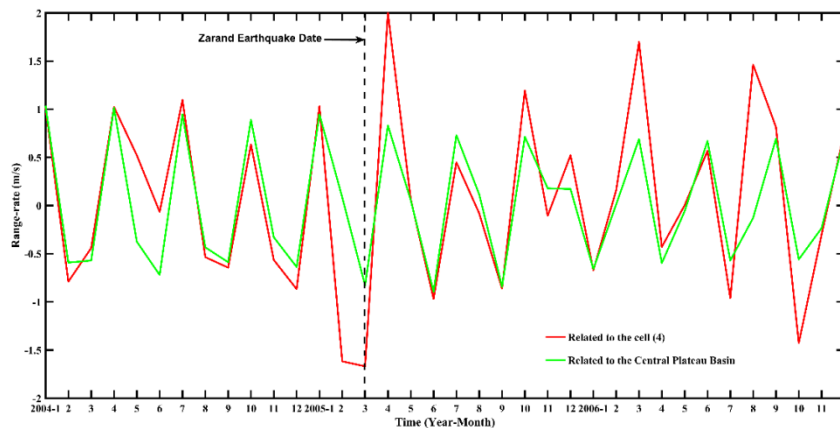


Figure 5. Corrected monthly range-rate time series related to cell (4) and the Central Plateau basin from the beginning of 2004 to the end of 2006.

For a more detailed analysis of the time series shown in Figures 4 and 5, the signals' details are extracted using the discrete wavelet transform (Burrus, 1997). According to wavelet terminology, a function $f(t)$ can be represented as a weighted summation as follows (Burrus, 1997):

$$f(t) = \sum_{k=-\infty}^{+\infty} c_k \varphi_k(t) + \sum_{k=-\infty}^{+\infty} \sum_{j=0}^{+\infty} d_{j,k} \psi_{j,k}(t) \quad (4)$$

where, $\psi_{j,k}(t)$ are the wavelets constructed by translating and stretching a main producer function $\psi(t)$, known as mother wavelet as follows:

$$\psi_{j,k}(t) = \psi(2^j t - k) \quad (5)$$

and $\varphi_k(t)$ are known as scaling functions, which are the translated versions of a basic scaling function $\varphi(t)$ as:

$$\varphi_k(t) = \varphi(t - k) \quad (6)$$

The expansion coefficients c_k and $d_{j,k}$ in Equation (4) are called the discrete wavelet transform (DWT) of the signal $f(t)$.

In Equation (4), the first part contains the coarse information about the function, and the remaining details are reflected in the second part.

According to the wavelet transform as a multiresolution analysis, introduced by Mallat (1989) and improved by Beylkin et al. (1991), the fast and simple implementation of discrete wavelet transform and its inverse is equivalent to using highpass and lowpass filters with impulse responses $h(n)$ and $g(n)$, respectively. These filters are related to each other as (Li, 1996):

$$g(n) = (-1)^{n-1} h(-n - 1) \quad (7)$$

From this point of view, the wavelet-based decomposition and reconstruction of a uniformly sampled function $\{f_{i+1}(n), n \in Z\}$, can respectively be computed as follows (Li, 1996):

$$\begin{cases} c_i(n) = \sum_k h(2n - k) f_{i+1}(k) \\ d_i(n) = \sum_k h(2n - k) f_{i+1}(k) \end{cases} \quad (8)$$

and

$$f_{i+1}(n) = \sum_k h(2k - n) c_i(k) + \sum_k g(2k - n) d_i(k) \quad (9)$$

By applying the one-dimensional discrete wavelet transform to the range-rate time series shown in Figures 4 and 5, their corresponding details are shown in Figures 6 and 7. Figures 6 and 7 also show the lower and upper limits of the extracted details (the red lines), based on the boxplot method. In this procedure, the lower and upper limits of a data set are defined based on the median of the lower and upper halves of the data set as the first and the third quartiles, respectively. The difference between the first quartile (Q1) and the third quartile (Q3) is considered as interquartile range (IQR). Observations that fall below the lower limit ($Q_1 - 1.5 \times IQR$) or above the upper limit ($Q_3 + 1.5 \times IQR$) are potential outliers, with an error risk of about 5% (Smiti, 2020).

In each signal in Figures 6 and 7, corresponding to the extracted details of the range-rate time series, the abnormal observations detected using the boxplot method may be considered as potential range-rate changes due to the impact of the earthquakes under study.

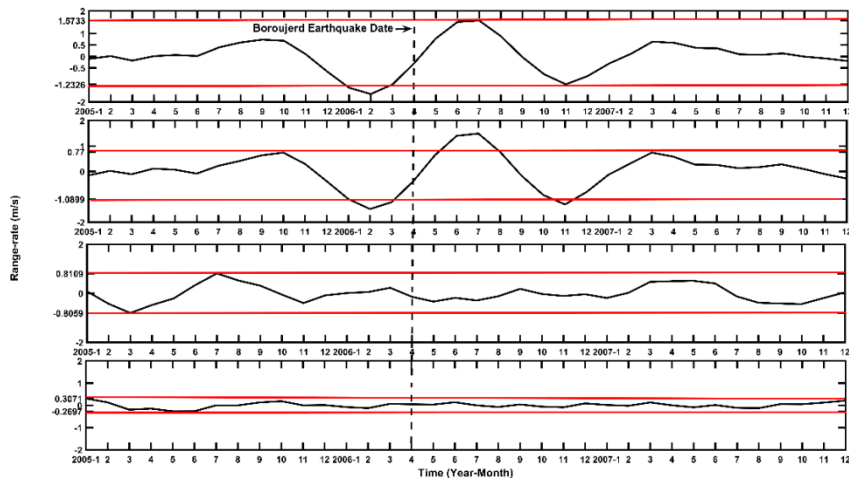


Figure 6. The details of the monthly corrected GRACE range-rate time series obtained from the application of discrete wavelet transform on the range-rate time series in Figure 4, top to bottom: related to the cells (1) to (3) and the Persian Gulf basin, respectively. The red lines show the first and third quartiles of the extracted details, based on the boxplot method.

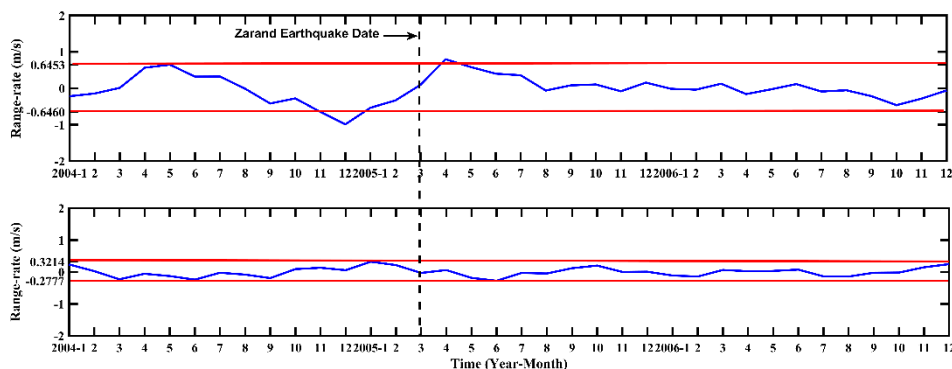


Figure 7. The details of the monthly corrected GRACE range-rate time series obtained from the application of discrete wavelet transform on the range-rate time series in Figure 5, top to bottom: related to cell (4) and the Central Plateau basin, respectively. The red lines show the first and third quartiles of the extracted details, based on the boxplot method.

As expected, according to Figures 6 and 7, the behavior of the detailed signals related to each of the four 1° square cells in Figure 1, is different from that of their corresponding catchment areas due to the nature of the GRACE range-rate observations. However, the more remarkable point in Figures 6 and 7 is the occurrence of outliers in the detailed signals corresponding to the cells containing the selected earthquakes' epicenters (cells 1 and 4), as well as cell 2, which is located near the epicenter of the Borujerd earthquake, while such outliers are no longer detectable in the detailed time series related to cell 3, where no earthquake occurred during the study period, as not seen in the Persian Gulf and the Central Plateau basins' details.

3. Conclusions

In this study, the behavior of GRACE level1B range-rate measurements under the influence of strong earthquakes was investigated, and this was contrary to the usual procedures in which the signals corresponding to the variable part of the Earth's gravity field extracted from GRACE, were used as conventional formats, such as spherical harmonic coefficients, which could lead missing information during the smoothing process.

After correcting the effect of the factors that led to the temporal variations of these observations, apart from hydrology and earthquakes, the reduced monthly range-rate time series related to four selected $1^\circ \times 1^\circ$ cells, as well as their corresponding catchment areas, were analyzed using the discrete wavelet transform and boxplot method. The results indicate that the behavior

of the reduced GRACE range-rate time series changes significantly in the cells containing or adjacent to the epicenter and at times around the moment of occurrence of the studied earthquakes.

It is suggested that other related GRACE level 1B data be examined to analyze the impact of strong earthquakes. Moreover, changing the dimensions of selected cells to extract time series at intervals of less than one month, as well as analyzing unevenly spaced time series made from instantaneous reduced range-rate measurements, may be helpful. In addition, when developing applications for wavelet transform, as an example, the effect of using or designing different base functions on the results can be investigated.

Considering the continuation of GRACE in the form of the GRACE Follow-On (GRACE-FO) mission (Kornfeld et al., 2019), the analysis of time and space series related to the first level of this mission, along with other available information sources, can provide significant and useful information about strong earthquakes.

References

- Barkat, A., Ali, A., Rehman, K., Awais, M., Riaz, M. S., & Iqbal, T. (2018). Thermal IR satellite data application for earthquake research in Pakistan. *Journal of Geodynamics*, 116, 13-22.
- Bezděk, A. (2010). Calibration of accelerometers aboard GRACE satellites by comparison with POD-based non-gravitational accelerations. *Journal of Geodynamics*, 50(5), 410-423.
- Burrus, C. S. (1997). Introduction to wavelets

- and wavelet transforms: a primer. *Englewood Cliffs*.
- Case, K., Kruizinga, G., & Wu, S.C. (2010). GRACE Level 1B Data Product User Handbook. *JPL D-22027*.
- Chen, J., Cazenave, A., Dahle, C., Llovel, W., Panet, I., Pfeffer, J., & Moreira, L. (2022). Applications and Challenges of GRACE and GRACE Follow-On Satellite Gravimetry. *Surveys in Geophysics*, 1-41.
- Chen, Y. (2007). *Recovery of terrestrial water storage change from low-low satellite-to-satellite tracking* (Doctoral dissertation, The Ohio State University).
- Choudhury, S., Dasgupta, S., Saraf, A. K., & Panda, S. (2006). Remote sensing observations of pre-earthquake thermal anomalies in Iran. *International Journal of Remote Sensing*, 27(20), 4381-4396.
- Dumka, R. K., SuriBabu, D., Malik, K., Prajapati, S., & Narain, P. (2020). PS-InSAR derived deformation study in the Kachchh, Western India. *Applied Computing and Geosciences*, 8, 100041.
- Ghobadi-Far, K., Han, S.C., Allgeyer, S., Tregoning, P., Sauber, J., Behzadpour, S., Mayer-Gürr, T., Sneeuw, N., & Okal, E. (2020). GRACE gravitational measurements of tsunamis after the 2004, 2010 and 2011 great earthquakes. *Journal of Geodesy*, 94(7), 1-9.
- Han, S. C., Sauber, J., & Luthcke, S. (2010). Regional gravity decrease after the 2010 Maule (Chile) earthquake indicates large-scale mass redistribution. *Geophysical Research Letters*, 37(23).
- Han, S. C., Sauber, J., & Riva, R. (2011). Contribution of satellite gravimetry to understanding seismic source processes of the 2011 Tohoku-Oki earthquake. *Geophysical Research Letters*, 38(24).
- Han, S. C., Shum, C. K., Bevis, M., Ji, C., & Kuo, C. Y. (2006). Crustal dilatation observed by GRACE after the 2004 Sumatra-Andaman earthquake. *Science*, 313(5787), 658-662.
- Kornfeld, R. P., Arnold, B. W., Gross, M. A., Dahya, N. T., Klipstein, W. M., Gath, P. F., & Bettadpur, S. (2019). GRACE-FO: the gravity recovery and climate experiment follow on mission. *Journal of spacecraft and rockets*, 56(3), 931-951.
- Larkina, V. I., Nalivayko, A. V., Gershenson, N. I., Gokhberg, M. B., Liperovskiy, V. A., & Shalimov, S. L. (1983). Observations of VLF emission, related with seismic activity, on the Interkosmos-19 satellite. *Geomagnetism and Aeronomy*, 23(5), 684.
- Liu, F., Elliott, J. R., Craig, T. J., Hooper, A., & Wright, T. J. (2021). Improving the resolving power of InSAR for earthquakes using time series: a case study in Iran. *Geophysical Research Letters*, 48(14), e2021GL093043.
- Moradi, A., & Sharifi, M. A. (2017). Windowed least-squares spectral analysis of grace K- band range rate measurements. *Appl. Ecology Env. Res*, 15(1), 429-437.
- Moradi, A., & Sharifi, M. A. (2018). Wavelet analysis of GRACE K-band range rate measurements related to Urmia Basin. *Iranian Journal of Geophysics*, 11(5), 43-54.
- Moradi, A., & Sharifi, M. A. (2021). Calibration of the accelerometers on board GRACE satellites using discrete wavelet transform. *Iranian Journal of Geophysics*, 15(4), 29-36.
- Nardò, S., Ascione, A., Mazzuoli, S., Terranova, C., & Vilardo, G. (2020). PS-InSAR data analysis: pre-seismic ground deformation in the 2009 L'Aquila earthquake region. *Bollettino di Geofisica Teorica ed Applicata*, 61(1), 41-56.
- Panet, I., Mikhailov, V., Diament, M., Pollitz, F., King, G., De Viron, O., Holschneider, M., Biancale, R., & Lemoine, J.M. (2007). Coseismic and post-seismic signatures of the Sumatra 2004 December and 2005 March earthquakes in GRACE satellite gravity. *Geophysical Journal International*, 171(1), 177-190.
- Pavlis, N.K., Holmes, S.A., Kenyon, S.C. and Factor, J.K. (2008) An Earth Gravitational Model to Degree 2160: EGM2008. Presented at the EGU General Assembly, Vienna Austria, April 13-18.
- Paziewski, J., Kurpinski, G., Wielgosz, P., Stolecki, L., Sieradzki, R., Seta, M., Oszczak, S., Castillo, M., & Martin-Porqueras, F. (2020). Towards Galileo+ GPS seismology: Validation of high-rate GNSS-based system for seismic events characterization. *Measurement*, 166, 108236.
- Petit, G., & Luzum, B. (2010). *IERS conventions (2010)*. Bureau International

- des Poids et mesures sevrés (France).
- Pulinets, S. (2004). Ionospheric precursors of earthquakes; recent advances in theory and practical applications. *Terrestrial Atmospheric and Oceanic Sciences*, 15(3), 413-436.
- Pulinets, S. A., Gaivoronska, T. B., Leyva Contreras, A., & Ciraolo, L. (2004). Correlation analysis technique revealing ionospheric precursors of earthquakes. *Natural Hazards and Earth System Sciences*, 4(5/6), 697-702.
- Ramazi, H., & Hosseinnejad, M. (2009). The Silakhor (Iran) earthquake of 31 March 2006, from an engineering and seismological point of view. *Seismological Research Letters*, 80(2), 224-232.
- Rummel, R., Balmino, G., Johannessen, J., Visser, P. N. A. M., & Woodworth, P. (2002). Dedicated gravity field missions—principles and aims. *Journal of Geodynamics*, 33(1-2), 3-20.
- Saatsaz, M. (2020). A historical investigation on water resources management in Iran. *Environment, Development and Sustainability*, 22(3), 1749-1785.
- Saraf, A. K., Rawat, V., Choudhury, S., Dasgupta, S., & Das, J. (2009). Advances in understanding of the mechanism for generation of earthquake thermal precursors detected by satellites. *International Journal of Applied Earth Observation and Geoinformation*, 11(6), 373-379.
- Shahrisvand, M., Akhoondzadeh, M., & Sharifi, M. A. (2014). Detection of gravity changes before powerful earthquakes in GRACE satellite observations. *Annals of Geophysics*, 57(5), 0543.
- Smiti, A. (2020). A critical overview of outlier detection methods. *Computer Science Review*, 38, 100306.
- Su, L. N., Gan, W. J., & Xiao, G. R. (2018). Brief overview on high-rate GPS epoch-by-epoch precise positioning and GPS seismology. *Progress in Geophysics*, 33(2), 503-510.
- Swenson, S., & Wahr, J. (2006). Post-processing removal of correlated errors in GRACE data. *Geophysical research letters*, 33(8).
- Wells, D. E., Vaníček, P., & Pagiatakis, S. D. (1985). Least squares spectral analysis revisited.
- Wyss, M. (1997). The second round of evaluations of proposed earthquake precursors. *Pure and Applied Geophysics*, 149(1), 3-16.
- Xiang, Y., Yue, J., Tang, K., & Li, Z. (2019). A comprehensive study of the 2016 Mw 6.0 Italy earthquake based on high-rate (10 Hz) GPS data. *Advances in Space Research*, 63(1), 103-117.
- Xu, P., Shi, C., Fang, R., Liu, J., Niu, X., Zhang, Q., & Yanagidani, T. (2013). High-rate precise point positioning (PPP) to measure seismic wave motions: an experimental comparison of GPS PPP with inertial measurement units. *Journal of Geodesy*, 87(4), 361-372.
- Zeng, Z. C., Zhang, B., & Fang, G. Y. (2009). The analysis of ionospheric variations before Wenchuan earthquake with DEMETER data. *Chinese J. Geophys.*
- Zhao, X., Pan, S., Sun, Z., Guo, H., Zhang, L., & Feng, K. (2021). Advances of satellite remote sensing technology in earthquake prediction. *Natural Hazards Review*, 22(1), 03120001.
- Zhong, M., Shan, X., Zhang, X., Qu, C., Guo, X., & Jiao, Z. (2020). Thermal Infrared and Ionospheric Anomalies of the 2017 Mw 6.5 Jiuzhaigou Earthquake. *Remote Sensing*, 12(17), 2843.